ENVIRONMENTAL RESEARCH
LETTERS

CrossMark

OPEN ACCESS

RECEIVED
9 March 2023

REVISED
27 April 2023

ACCEPTED FOR PUBLICATION
10 May 2023

PUBLISHED
26 May 2023

Original content from this work may be used under the terms of the Creative Commons Attribution 4.0 licence.

Any further distribution of this work must maintain attribution to the author(s) and the title of the work, journal citation and DOI.

LETTER

Extending global river gauge records using satellite observations

Ryan M Riggs[1,*], **George H Allen**[2], **Jida Wang**[3], **Tamlin M Pavelsky**[4], **Colin J Gleason**[5], **Cédric H David**[6] and **Michael Durand**[7]

[1] Department of Geography, Texas A&M University, College Station, TX, United States of America
[2] Department of Geosciences, Virginia Polytechnic Institute and State University, Blacksburg, VA, United States of America
[3] Department of Geography and Geospatial Sciences, Kansas State University, Manhattan, KS, United States of America
[4] Department of Geological Sciences, University of North Carolina, Chapel Hill, NC, United States of America
[5] Department of Civil and Environmental Engineering, University of Massachusetts, Amherst, MA, United States of America
[6] Jet Propulsion Laboratory, California Institute of Technology, Pasadena, CA, United States of America
[7] School of Earth Sciences, The Ohio State University, Columbus, OH, United States of America
[*] Author to whom any correspondence should be addressed.

E-mail: rriggs@tamu.edu

Keywords: river discharge, river gauge, remote sensing of discharge, rating curve, Landsat, Sentinel-2

Supplementary material for this article is available online

Abstract

Long-term, continuous, and real-time streamflow records are essential for understanding and managing freshwater resources. However, we find that 37% of publicly available global gauge records ($N = 45\,837$) are discontinuous and 77% of gauge records do not contain real-time data. Historical periods of social upheaval are associated with declines in gauge data availability. Using river width observations from Landsat and Sentinel-2 satellites, we fill in missing records at 2168 gauge locations worldwide with more than 275 000 daily discharge estimates. This task is accomplished with a river width-based rating curve technique that optimizes measurement location and rating function (median relative bias = 1.4%, median Kling-Gupta efficiency = 0.46). The rating curves presented here can be used to generate near real-time discharge measurements as new satellite images are acquired, improving our capabilities for monitoring and managing river resources.

1. Introduction

Since the turn of the 20th century, river gauges have provided critical river discharge measurements across much of the world (Murphy 1904). Long-term gauge records provide a baseline for understanding changes in water resources caused by climate change (Milly and Dunne 2020) and land use change (Gerten *et al* 2008), including human modifications of river corridors (Remo *et al* 2012). River gauges also produce the raw information needed to inform water resource management and thus often form the basis of water usage treaties (Drieschova *et al* 2008, Gerlak *et al* 2011, Dawadi and Ahmad 2012). Yet most publicly available global gauge records are not immediately available, do not extend to the present, and are often discontinuous (Do *et al* 2018).

High-latency and incomplete gauge records have real-world consequences. When near-real-time (NRT) gauge data are available, they are useful for early flood warning systems and other NRT water resource management applications (Gourley *et al* 2013, Bates *et al* 2021). Inaccessible NRT gauge data hampers understanding of rivers at the global scale and also the development of gauge-constrained hydrological products at an application-relevant latency (National Water Model 2016). Further, many global gauge records contain missing measurements, often due to instrument error or government restrictions on data access (Hannah *et al* 2011). For instance, 69% of the 30 959 gauge records in the global streamflow indices and metadata (GSIM) archive contain missing measurements (Do *et al* 2018, Gudmundsson *et al* 2018). Further, incomplete gauge records exacerbate the placement bias of gauge networks (Krabbenhoft *et al* 2022). This spatial and temporal paucity of gauge data has motivated alternative approaches for observing discharge at large scales.

© 2023 The Author(s). Published by IOP Publishing Ltd

Satellite remote sensing of discharge can be used to address the shortcomings of gauge records (Smith 1997). To date, more than a dozen studies have focused on building rating curves between satellite river observations and gauge measurements (Gleason and Durand 2020). Rating curves represent an empirical relationship between an observable river parameter (e.g. width, water surface elevation) and river discharge. These rating curves can then be used to estimate discharge from the observable river parameter alone. Using optical imagery from satellite missions and sensors including, Landsat, Sentinel-2, and the Moderate Resolution Imaging Spectroradiometer, several studies have paired satellite widths with gauge records to develop width-based rating curves (Smith and Pavelsky 2008, Pavelsky 2014, Feng *et al* 2019). Radar altimetry data has also been used to develop elevation-based rating curves in gauged reaches (Kouraev *et al* 2004, Getirana and Peters-Lidard 2013, Tourian *et al* 2013, Paris *et al* 2016). Unlike optical sensors, radar altimeters can collect data at night and during cloudy conditions but they currently have a relatively coarse spatial resolution, limiting river elevation measurements only to very wide rivers (Birkett *et al* 2002, Birkinshaw *et al* 2010, Coss *et al* 2020, Nielsen *et al* 2022). Rating curves can also be developed by pairing surface reflectance with gauge records (Brakenridge *et al* 2012, Hou *et al* 2018, Tarpanelli *et al* 2013, Tarpanelli and Domeneghetti 2021), but use of surface reflectance alone prevents integration of observations from other sensors into the rating curves.

Once developed, rating curves can provide valuable discharge information for water management purposes. For example, rating curves are capable of providing NRT discharge estimates where gauge data are unavailable (Riggs *et al* 2022). In addition, rating curves can supplement missing historic gauge measurements (Tourian *et al* 2017), improving our understanding of hydrological trends. Though numerous rating curve studies exist, they are typically limited to individual reaches or regions, making it difficult to assess their accuracy and usability at a broader scale (Huang *et al* 2018). Further, comparing rating curve approaches is difficult because many studies rely on different performance metrics. In this study, we compile the largest known dataset of publicly available river gauge data and analyze the temporal gaps of the compiled dataset. We then develop, assess the accuracy, and apply satellite-based rating curves to fill in the temporal gaps of gauge records.

2. Methods

2.1. Compiling and analyzing global gauge data

Here we collect and assess daily gauge data from a combination of international and national organizations to build an extensive global gauge database (table 1). We remove gauges located within ∼100 m of each other, assuming that they are redundant with one another (after Crochemore *et al* (2020), see table S1 for further information). All gauge databases used in this study are publicly available through a variety of web interfaces except for the Chinese Hydrology Project gauge data, which comprises less than 1% of gauges in this study. We assess the compiled gauge database to better understand spatial and temporal trends in gauge availability at the continental and global scales from 1900–2021. Specifically, we assess the number of operating gauges (with ⩾335 daily measurements in a given year) (U.S. Geological Survey 2019) and the proportion of operating gauges (the ratio of N operating gauges to N gauges ever installed) per year. We define gauge availability as the number of operating gauges per year. We also investigate trends in missing gauge measurements, by developing and applying a metric termed gauge record completeness (GRC) which is defined as,

$$\mathrm{GRC}\,(\%) = \left(\sum_{i}^{N_g} Nv_i / \sum_{i}^{N_g} Np_i\right) \times 100\% \qquad (1)$$

where N_g represents the number of gauges, Nv represents the number of valid measurements, and Np represents the number of days between the earliest and most recent valid discharge measurement for gauge i. We compare our findings with the 8187 gauge records containing daily discharge measurements in the Global Runoff Data Centre (GRDC) database (The Global Runoff Data Centre 2022). The GRDC is used for comparison with our compiled gauge database as it represents the largest collection of publicly accessible global gauge records.

2.2. Remote sensing of river widths

Because our technique combines same-day gauge discharge and satellite width measurements, we only use gauge records containing discharge measurements after the launch of Landsat 5 (1 March 1984), the earliest satellite used in this study. As gauge stations are often located on narrow, stable reaches (Park 1977), we consider locations upstream and downstream of gauges to determine the most suitable site for developing a width-based rating curve. These locations (hereinafter referred to as nodes) and the corresponding widths are from the Surface Water and Ocean Topography (SWOT) River Database (SWORD) (Altenau *et al* 2021) and represent locations where SWOT is expected to provide river observations at ∼200 m spacing. The SWORD mean width attribute is derived from river width measurements at mean discharge (Allen and Pavelsky 2018), which correspond on average to mean width (Allen *et al* 2020). We limit the analysis to gauges with at least one SWORD node mean width ⩾120 m (after Ishitsuka *et al* 2021) within a 2 km Euclidean radius and a 10 km river network distance (figure 1(a)). As

Table 1. Gauge data sources used in this analysis (see references for URLs).

Reference	*N* gauges	Record start–end	Date of access	*N* days extended (filled in)
ArcticNET (2022)	116	1913–2003	05/2021	1734 (86)
Australian Bureau of Meteorology (2022)	4340	1899–2021	09/2021	10 789 (1625)
Brazil National Water Agency (2022)	1342	1920–2021	09/2021	17 769 (5465)
Canada National Water Data Archive (2022)	6066	1860–2021	10/2021	27 758 (4073)
Chile Center for Climate and Resilience Research (2022)	501	1913–2020	09/2021	2639 (622)
Chinese Hydrology Project (Henck *et al* 2010, Schmidt *et al* 2011)	141	1953–1987	09/2021	0 (0)
The Global Runoff Data Centre (2022)	6614	1806–2021	09/2021	96 009 (7782)
India Water Resources Information System (2022)	549	1960–2020	06/2021	2345 (464)
Japanese Water Information System (2022)	1023	1954–2019	09/2021	9155 (1,556)
Spain Anuario de Aforos (2022)	1385	1912–2018	09/2021	13 758 (813)
Thailand Royal Irrigation Department (2022)	126	1980–1999	09/2021	4175 (202)
U.S. Geological Survey (2022)	23 634	1857–2021	09/2021	60 021 (11 097)

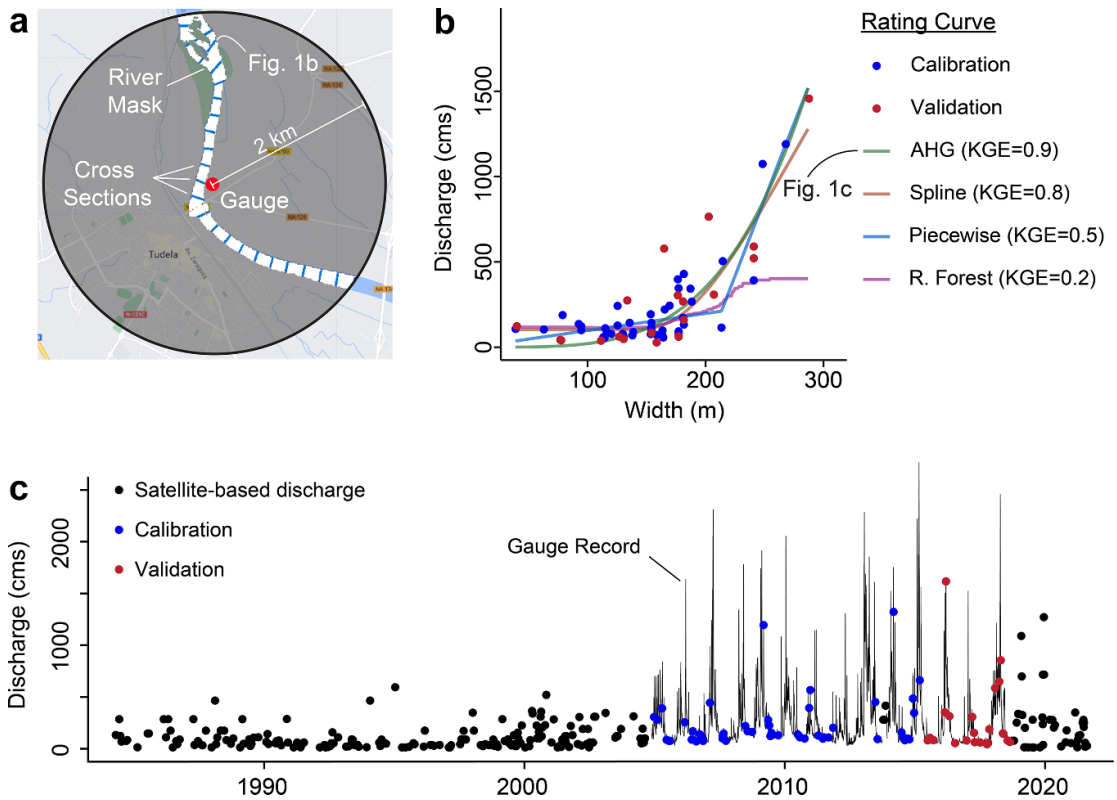

Figure 1. Width-based rating curve method for a high performing example gauge location along the Ebro River, Spain (Gauge agency ID: Spain Annuario de Aforos; Gauge ID: 9284_AFD). (a) Example river mask (white) clipped with 2 km gauge buffer with wetted node widths (blue). (b) Rating curves generated for one example SWORD node. (c) Gauge record supplemented with satellite observations using the highest performing node location (shown in a) and function (shown in b).

some gauges lie on nearby tributaries, we further limit the analysis to gauges with a mean discharge ⩾20 cubic meters per second (cms) because, on average, this discharge corresponds to the minimum discharge for a river with a mean width ⩾120 m (Frasson *et al* 2019) (table S1). To calculate river widths, we use Google Earth Engine (Gorelick *et al* 2017) and a modified version of RivWidthCloud (Yang *et al* 2020) to process Landsat-5, 7, 8 (30 m spatial resolution) and Sentinel-2 (10 m spatial resolution) imagery from 1

March 1984 to 27 August 2021 (see text S1 for more information).

2.3. Rating curve functions

We pair same-day gauge discharge with satellite width measurements at each node to develop four types of rating curve functions (figure 1(b)), further increasing the number of candidate rating curves for each gauge. The four rating curve types are at-a-station hydraulic geometry (AHG) (i.e. power-law function) (Leopold and Maddock 1953), piecewise linear regression (Lewis 1966, Mersel *et al* 2013, Elmi *et al* 2021), monotonic spline (Clarke *et al* 2000), and random forest (Kumar *et al* 2020). We select these four diverse function types because they are common approaches with their own respective strengths and weaknesses (see code repository for function parameterization). To eliminate unrealistic rating curves, we remove individual rating curves that do not exhibit an overall positive relationship between width and discharge. In total, 145 232 rating curves are developed and 52 178 rating curves are flagged for errors or insufficient training data and removed (see table S1 for more information).

We use the oldest 70% of the paired width-discharge data to calibrate the rating curves and use the remaining paired data for validation. We assess the performance of all node-level rating curves using the Kling-Gupta efficiency (KGE) (see table S2 for error metric equations) (Gupta *et al* 2009) and designate the highest performing node-level rating curve as the rating curve for that gauge (figure 1(c)). For example, if there are 20 viable SWORD nodes for a single gauge, 80 rating curves are generated (20 SWORD nodes $\times$ 4 rating curve types) and only the highest performing rating curve would be used for supplementing the gauge record. We apply the commonly used KGE for the rating curve assessment because its performance integrates both model variability and bias in a more balanced manner than similar metrics such as the Nash Sutcliffe efficiency (Nash and Sutcliffe 1970, Gupta *et al* 2009). To compare the performance of our remote sensing approach to the performance of a global hydrologic model, we compare our rating curves to the Global Reach-level *A priori* Discharge Estimates for SWOT (GRADES) hydrological model which contains daily discharge estimates at 2.94 million river reaches from 1979–2014 (Lin *et al* 2019). We select GRADES for comparison because it will provide *a priori* discharge estimates for the SWOT discharge product and we seek to determine whether this study's rating curves could be used to improve upon these *a priori* discharge estimates.

3. Results

3.1. Gaps in the global gauge record

Analyzing a total of 45 837 global river gauge records, we characterize the spatial and temporal trends of global river gauge availability (figures 2 and S1). We find that global gauge availability (N operating gauges) increased from 1900 until the 1980s and has since remained relatively stable (figure 2(b)). However, this global trend in gauge availability is largely dictated by the North American data because this region contains 67% of the gauges in our database followed by Oceania (10%), Europe (9%), Asia (6%), South America (5%), and Africa (3%). At the continental scale, we find that North American gauge availability has remained relatively steady since $\sim$1980 whereas Asia, Oceania, and South America steadily increase in gauge availability over time (figure 3). Conversely, from 1980 to 2015, African and European gauge availability declined by 47% and 20%, respectively.

Similarly, we find that the proportion of operating gauges (the ratio of N operating gauges to N gauges ever installed) tends to increase over time on most continents with the exception of Africa and Europe which have seen a declining proportion since the 1980s (figure 3). We also investigate instances of missing gauge measurements to understand the causes of gauge record fragmentation. Globally, the median duration a gauge is offline is five consecutive days, which could lead to missed observations of important flow events such as floods. Gauges go offline a median of once throughout their lifespan with the median number of offline events per gauge higher in Africa (10) and South America (8) than in Oceania (3), Asia (3), Europe (1) or North America (1). Across all gauges, the global GRC (equation 1) is 86%. At the continental scale, we find that GRC is less in Africa (87%), Asia (87%), and North America (84%) than in Europe (92%), Oceania (91%), and South America (91%) (figure 3).

GRC tends to increase over time, with periodic declines that often occur during socially turbulent time periods (figure 3). We emphasize that these findings represent correlation and not necessarily causation between historic events and GRC. Our gauge analysis is performed at the continental to global scale so we cannot justify making inferences related to individual countries' political and social history. Thus, the following is not an exhaustive list but rather a broad continental-scale overview of coinciding chaotic historical events and declines in GRC. We base our historical analysis on the work of Findley and Rothney (2011) which provides detailed information on the history of the 20th century. African GRC decreases from 1939–1945 (two-sample, one-sided Welch's t-test $p < 0.001$) and from 1988–1991 ($p < 0.05$) which is in accordance with World War II and the dissolution of the Soviet Union, respectively. Asian GRC improves for much of the time series with periodic decreases from 1939–1945 ($p < 0.05$) and the 1970s which aligns with World War II and Southeast Asian wars, respectively. European GRC shows three distinct declines: 1914–1918 ($p < 0.001$), 1929–1945

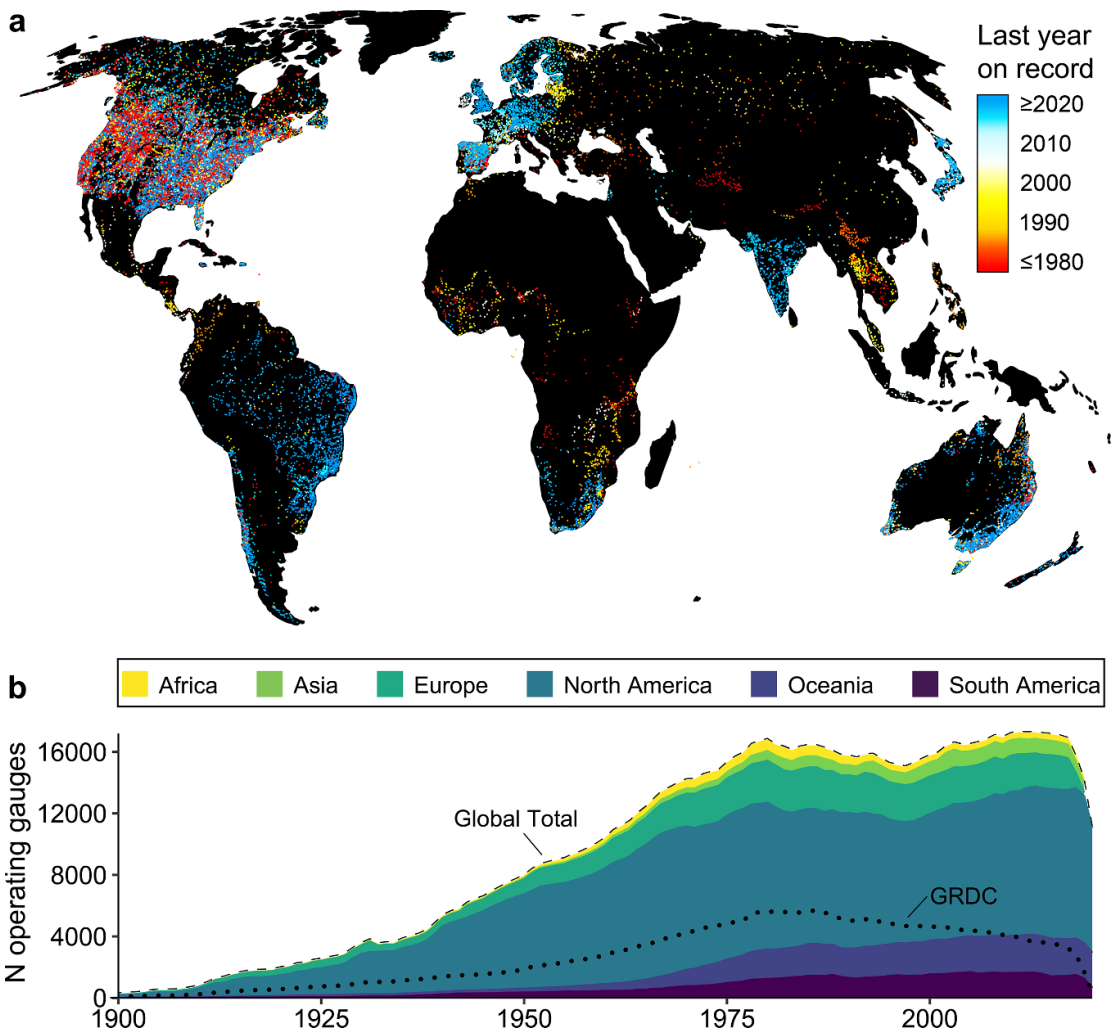

Figure 2. Publicly available gauge records analyzed by this study ($N = 45\,837$ gauges). (a) Map showing the last year on record of the accessed gauge records (accessed from 15 June 2021–22 October 2021). (b) Stacked area plot of publicly available daily gauge observations and the number of operating gauges available per year for each continent compared with the GRDC database ($N = 8187$ gauges).

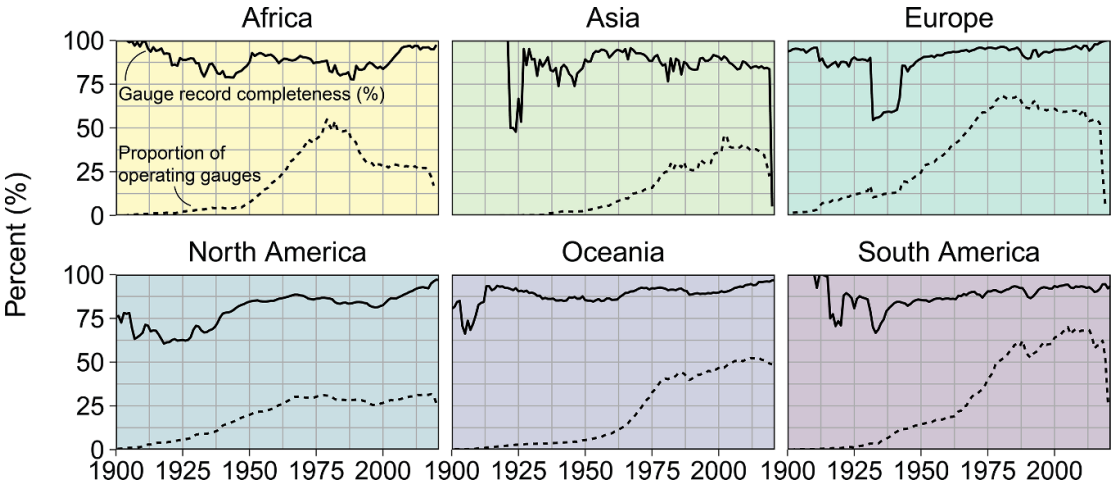

Figure 3. Continental gauge record trends. Gauge record completeness (solid line) and proportion of operating gauges (dashed line) for each continent.

($p < 0.001$), and 1988–1991 ($p < 0.001$). These declines in European GRC occur simultaneously with World War I, the Great Depression coupled with the Spanish Civil War and World War II, and the Soviet Union's breakup. North American, Oceanian, and South American GRC broadly increase over time with a decline in North and South American GRC from 1929–1939 ($p < 0.001$), which is in sync with the great depression. Across nearly all continents, we find that most large dips in GRC correlate with tumultuous historical events.

3.2. Supplementing global gauge records with satellite observations

To fill in gaps in the global gauge record with satellite measurements, we identify 2168 gauges that meet the requirements discussed in section 2.2. We use an average of 111 paired width-discharge data to calibrate the rating curves ($N = 240\,735$) with an average of 48 paired data for rating curve validation ($N = 103\,246$). The optimal node-level rating curve is often located some distance from the gauge location (mean streamwise distance of 1281 m) and we find that upstream and downstream nodes perform equally well. Of the optimal rating curve fit at each gauge, our technique selects AHG the most frequently (60%), followed by monotonic spline (20%), piecewise linear regression (15%), and random forest (5%). AHG power-law rating curves have a mean a coefficient of 33 ± 53 (1-sigma variation) and a mean b exponent of 0.42 ± 0.22. We use RiverATLAS (Linke *et al* 2019) to assign Strahler stream order to each gauge and find that the proportion of AHG rating curves declines in stream orders greater than 6 (figure S2).

Applying our width-based rating curve approach to each of the 2168 gauges adds 279 937 daily discharge observations to global gauge records, where 246 152 of these discharge observations extend gauge records beyond their lifespan and 33 785 discharge observations fill historical gaps in gauge records (figure 4). Using the BasinATLAS Level 3 product (Linke *et al* 2019), we find that gauge records in arid environments (average annual precipitation/potential evapotranspiration <0.5) are filled in at a higher mean annual rate than in more humid regions (5.0 vs. 3.3 observations/gauge/year, respectively), likely due to a higher proportion of cloud-free imagery in arid environments (Ju and Roy 2008). The infilling rate is also impacted by the number of available satellite-based sensors during a given time period. From 2017 to 2021, the heightened availability of Sentinel-2 data combined with the dearth of more recent gauge data (figure 4(b)) quadruples the infilling rate to 26 094 observations/year. The decommissioning of satellites has the opposite effect, with the notable example of a major decrease in observations/year in 2012 due to instrument failures on Landsat 5 prior to the commissioning of Landsat 8 (Neigh 2021).

The rating curve approach presented here produces a median rBias of 1.4% (mean = 4.6%) and a median absolute rBias of 14% (mean = 21.5%), substantially lower than the typical bias produced from hydrological models (figure 4(c)). In addition, we find a median normalized root-mean-square error (NRMSE), relative root-mean-square error (RRMSE), and KGE of 63%, 83%, and 0.46, respectively. Ninety seven percent of the rating curves have a KGE >-0.41, implying that the vast majority of locations improve upon using the mean observed discharge for supplementing the gauge record (Knoben *et al* 2019). We find that rating curve performance remains relatively stable regardless of stream order (figure S3). We compare GRADES daily discharge to 2071 of the gauge records used in our analysis as these records overlap with the GRADES simulation data. As expected, we find that GRADES can supplement the global gauge record at a higher rate than our rating curve approach (figure 4(b)). However, our rating curve method outperforms GRADES across all gauges in terms of rBias, NRMSE and KGE, and particularly outperforms GRADES in arid regions (figures 4(c)–(e)). GRADES poor performance in arid regions has been attributed to inaccurate meteorological inputs (Beck *et al* 2015) and could also be related to the non-perennial and flashy nature of rivers in arid regions. In contrast, our rating curves are gauge-constrained and based on direct satellite observations, allowing them to estimate discharge without the need to model hydrological processes.

4. Discussion

In contrast to previous gauge availability studies that rely entirely on the GRDC (Hannah *et al* 2011) or use some but not all of the national organizations found in the GSIM database (Crochemore *et al* 2020), we do not find a decline in record availability (the number of operating gauges per year) over the last four decades (figure 2). These differences in findings are driven by newfound increases in gauge availability across much of Asia, Oceania and South America, as well as a less rapid decline in Europe since the 1980s. In Asia, an overall increase in continental gauge availability is contrasted by the absence of gauge data in China and Russia after 2004 and 2011, respectively. Further, the Asian gauge network is unevenly spatially distributed with only ~13% of Asian gauges located in China and Russia even though these countries cover approximately half of Asia's landmass. International gauge databases such as the GRDC have proved instrumental in providing access to global gauge data for hydrological studies (Addor *et al* 2020). However, pulling data directly from publicly available national agency websites is a promising way to improve data latency and coverage as international gauge databases are updated infrequently and are insufficient to

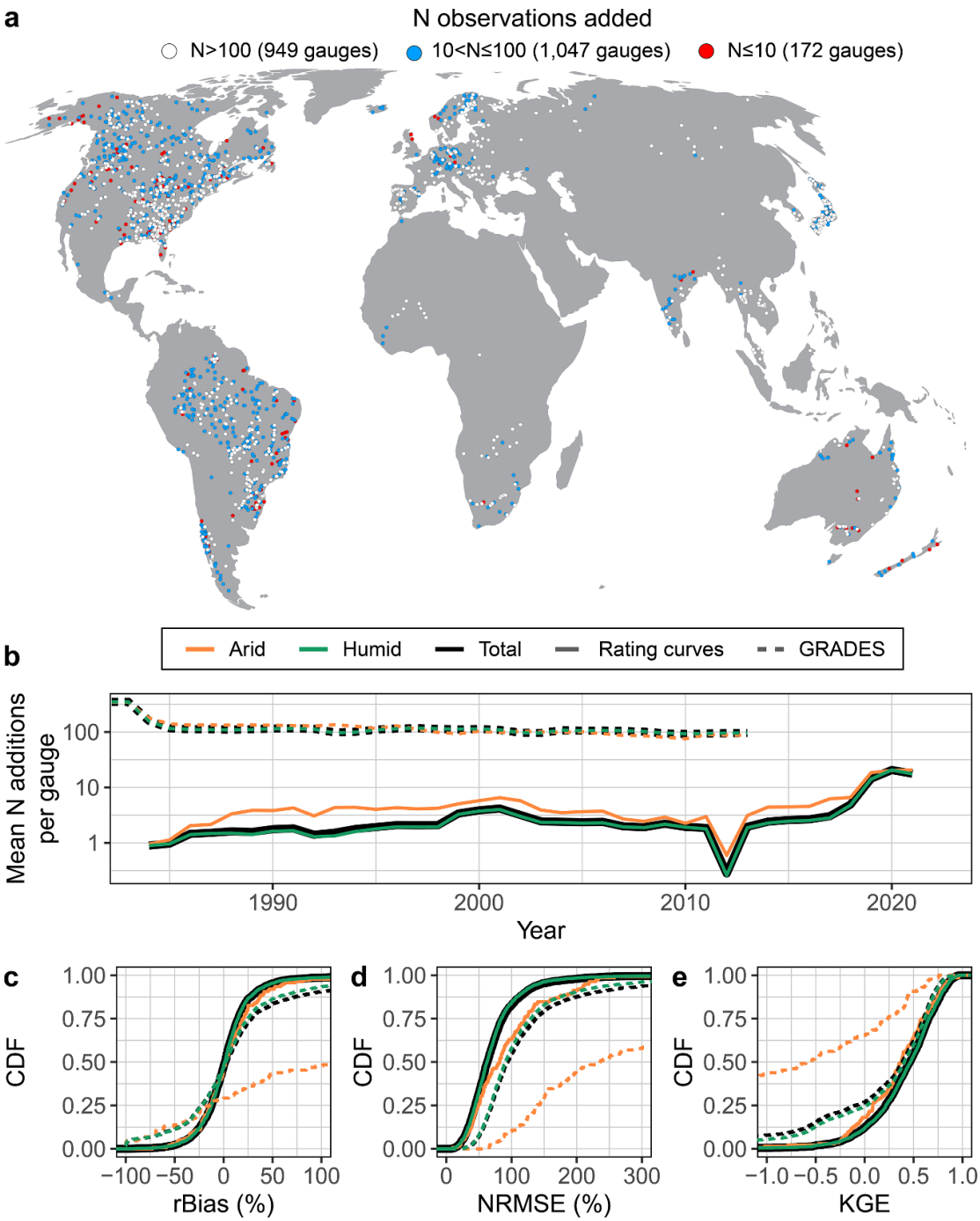

Figure 4. Spatial and temporal patterns of supplementing global gauge records using satellite observations. (a) Number of supplemented gauge record observations at all 2168 gauges. (b) Mean number of observations added per gauge/year. GRADES streamflow simulation is also shown (dashed line). Cumulative distribution functions for rBias (c), NRMSE (d), and KGE (e).

characterize the global availability of gauge records (figure 2(b)).

The rating curves developed here can be used to improve river flow measurement latency in large rivers with near-zero rBias on average. We find that our AHG *b* exponent values are within the range of other gauge-based AHG studies (Dingman 2007, Gleason 2015), which is likely related to gauges being preferentially placed along stable reaches (Allen and Pavelsky 2015). We speculate that human modifications along large rivers or fundamental differences in geomorphic scaling relationships (e.g. width/depth ratio) may be the reason for the decline in AHG performance in higher stream order rivers but future studies should explore this relationship further. As 77% of the gauge records collected here do not contain data within a month of access, low-latency satellite data (Landsat: 0–26 d, Sentinel-2: 0–7 d) can be used to improve the amount of NRT information on river flows (U.S. Geological Survey 2018, ESA 2022). For example, 30% of our satellite-based gauge record additions are from 2020 or 2021 which is driven by the lack of NRT gauge data. While hydrological models can also be used to supplement gauge records,

our rating curves outperform the GRADES hydrological model and produce a lower bias, on average, than several additional large-scale hydrological models (Zhao *et al* 2017, Harrigan *et al* 2020, Yang *et al* 2021). Although our rating curve approach has near-zero rBias on average and provides NRT data, it is unable to match the continuous temporal resolution and contiguous spatial coverage of hydrological models (figure 4(b)). Therefore, perhaps the best solution could be obtained by incorporating these rating curve based estimates into a hydrologic model through data assimilation.

The raw rating curves produced by this study can also be used in conjunction with additional satellite missions to further improve access to NRT discharge estimates. For instance, the SWOT satellite will provide global discharge estimates by combining SWOT river observations with gauge and theoretical information (Durand *et al* 2014, Feng *et al* 2021, Larnier *et al* 2021). The official SWOT discharge products require prior discharge estimates from historic gauge data or modeled discharge and performance is limited in places by high bias in the prior discharge estimates (Durand *et al* 2016, deFrasson *et al* 2021). Thus, our near-zero rBias rating curve approach is potentially advantageous for providing this critical prior information alongside modeled data from GRADES in these locations.

Although the rating curves presented here can provide valuable NRT information, there are limitations involved in the approach presented in this study. First, our rating curve technique is limited by the spatial resolution of the imagery used, restricting rating curve development to only ∼5% of publicly available gauges. The satellite optical sensors used in this study are inherently limited by cloud cover and nighttime conditions (King *et al* 2013). Thus, the implementation of SWOT or other radar observations into our rating curves will provide additional data for supplementing global gauge records at a greater temporal resolution. With the expected proliferation of satellite observations in the coming years (Rosen *et al* 2017, Blumstein *et al* 2019, Wulder *et al* 2019), future efforts could integrate river observations from a variety of available sensors and sensor types (optical, microwave, altimeters) to improve the spatial and temporal capabilities for supplementing global gauge records. Additional observations could be extracted from commercial satellite data (Stringham *et al* 2019, Ignatenko *et al* 2020, Kulu 2021). Ultimately, a multi-sensor approach for satellite remote sensing could serve to improve our understanding of global river discharge dynamics.

5. Conclusions

We find that satellite remote sensing can supplement global river gauge records by filling in temporal gaps and extending high-latency databases to NRT. In contrast to previous studies that largely rely on international gauge databases, our analysis of both national and international gauge databases indicates that global gauge availability is not declining but has been relatively stable since ∼1980. Specifically, we find that while gauge availability is decreasing on some continents (Africa and Europe), many continents are showing increases in the number of publicly available gauges (Asia, Oceania, and South America) or are remaining steady (North America) (figure 2). We find that gauges typically go offline for short periods (∼5 consecutive days) and a much larger percentage of missing measurements occurs during historical periods of social upheaval (figure 3). The rating curve technique presented here provides a near-zero bias and high KGE approach for providing historic and NRT discharge estimates, which can be used to fill in and extend gauge records (figure 4). Further, our rating curves can provide NRT access to discharge data, unavailable at 77% of gauges. Finally, the approach developed here can be used in conjunction with future satellite missions to significantly improve the spatial and temporal density of remotely sensed discharge data to further supplement global gauge records.

Data availability statement

The gauge database, supplemented gauge discharge data, and rating curves produced by this study are openly available on Zenodo (https://zenodo.org/record/7150168#.ZAow8RXMIuV) and the code used in this analysis can be found on GitHub (https://github.com/Ryan-Riggs/ExtendingGaugeRecords). The following gauge databases are publicly available: ArcticNet (www.r-arcticnet.sr.unh.edu/v4.0/AllData/index.html), Australian Bureau of Meteorology (www.bom.gov.au/waterdata/), Brazil National Water Agency (www.snirh.gov.br/hidroweb/serieshistoricas), Canada National Water Data Archive (www.canada.ca/en/environment-climate-change/services/water-overview/quantity/monitoring/survey/data-products-services/national-archive-hydat.html), Chile Center for Climate and Resilience Research (https://explorador.cr2.cl/), The Global Runoff Data Centre (https://portal.grdc.bafg.de/applications/public.html?publicuser=PublicUser), India Water Resources Information System (https://indiawris.gov.in/wris/#/RiverMonitoring), Japanese Water Information System (www1.river.go.jp/), Spain Annuario de Aforos (http://datos.gob.es/es/catalogo/e00125801-anuario-de-aforos/resource/4836b826-e7fd-4a41-950c-89b4eaea0279), Thailand Royal Irrigation Department (http://hydro.iis.u-tokyo.acjp/GAME-T/GAIN-T/routine/rid-river/disc_d.html), and the U.S. Geological Survey (https://waterdata.usgs.gov/nwis/rt). The Chinese Hydrology Project data is not publicly available and was provided by the authors of

the dataset (Henck *et al* 2010, Schmidt *et al* 2011). The GRADES hydrological model outputs are publicly available online (www.reachhydro.org/home/records/grades).

Acknowledgments

This work was supported by the NASA SWOT Science Team (NNH19ZDA001N-SWOTST), NASA's Terrestrial Hydrology Program (NNH17ZDA001N-THP), the Texas A&M Presidential Excellence Fund, and the Texas Space Grant Consortium. T M Pavelsky's work on this project was supported by a contract from the SWOT Project Office at the NASA/Caltech Jet Propulsion Lab. C H David was supported by the Jet Propulsion Laboratory, California Institute of Technology, under a contract with NASA.

ORCID iDs

Ryan M Riggs https://orcid.org/0000-0001-6834-9469
George H Allen https://orcid.org/0000-0001-8301-5301
Jida Wang https://orcid.org/0000-0003-3548-8918
Tamlin M Pavelsky https://orcid.org/0000-0002-0613-3838
Colin J Gleason https://orcid.org/0000-0002-3525-6220
Cédric H David https://orcid.org/0000-0002-0924-5907
Michael Durand https://orcid.org/0000-0003-2682-6196

References

Addor N, Do H X, Alvarez-Garreton C, Coxon G, Fowler K and Mendoza P A 2020 Large-sample hydrology: recent progress, guidelines for new datasets and grand challenges *Hydrol. Sci. J.* **65** 712–25

Allen G H and Pavelsky T M 2015 Patterns of river width and surface area revealed by the satellite-derived North American River width data set *Geophys. Res. Lett.* 42 395–402

Allen G H and Pavelsky T M 2018 Global extent of rivers and streams *Science* **361** 585–8

Allen G H, Yang X, Gardner J, Holliman J, David C H and Ross M 2020 Timing of Landsat overpasses effectively captures flow conditions of large rivers *Remote Sens.* **12** 1510

Altenau E H, Pavelsky T M, Durand M T, Yang X, Frasson R P D M and Bendezu L 2021 The surface water and ocean topography (SWOT) mission river database (SWORD): a global river network for satellite data products *Water Resour. Res.* **57** e2021WR030054

ArcticNET 2022 *ArcticNET V1.0* (available at: https://russia-arcticnet.sr.unh.edu/)

Australian Bureau of Meteorology 2022 *Australian Bureau of Meteorology* (available at: www.bom.gov.au/)

Bates P D *et al* 2021 Combined modeling of US fluvial, pluvial, and coastal flood hazard under current and future climates *Water Resour. Res.* **57** e2020WR028673

Beck H E, de Roo A and van Dijk A I J M 2015 Global maps of streamflow characteristics based on observations from several thousand catchments *J. Hydrometeorol.* **16** 1478–501

Birkett C M, Mertes L A K, Dunne T, Costa M H and Jasinski M J 2002 Surface water dynamics in the Amazon Basin: application of satellite radar altimetry *J. Geophys. Res. Atmos.* **107** LBA 26-1-LBA 26–21

Birkinshaw S J, O'Donnell G M, Moore P, Kilsby C G, Fowler H J and Berry P A M 2010 Using satellite altimetry data to augment flow estimation techniques on the Mekong River *Hydrol. Process.* **24** 3811–25

Blumstein D, Biancamaria S, Guérin A and Maisongrande P 2019 A potential constellation of small altimetry satellites dedicated to continental surface waters (SMASH mission) **2019** *American Geophysical Union Fall Meeting* (*San Francisco, California 2019*) H43N–2257 (available at: https://ui.adsabs.harvard.edu/abs/2019AGUFM.H43N2257B/abstract)

Brakenridge G R, Cohen S, Kettner A J, De Groeve T, Nghiem S V, Syvitski J P M and Fekete B M 2012 Calibration of satellite measurements of river discharge using a global hydrology model *J. Hydrol.* **475** 123–36

Brazil National Water Agency 2022 National water and sanitation agency (ANA) *Agência Nac Águas E Saneam. Básico ANA* (available at: www.gov.br/ana/en/national_water_agency)

C P C 1977 World-wide variations in hydraulic geometry exponents of stream channels: an analysis and some observations *J. Hydrol.* **33** 133–46

Canada National Water Data Archive 2022 National water data archive *HYDAT* (available at: www.canada.ca/en/environment-climate-change/services/water-overview/quantity/monitoring/survey/data-products-services/national-archive-hydat.html)

Chile Center for Climate and Resilience Research 2022 Center for climate and resilience research *CR2 | Chilean research center on climate, climate change and resilience* (available at: www.cr2.cl/eng/)

Clarke R T, Mendiondo E M and Brusa L C 2000 Uncertainties in mean discharges from two large South American rivers due to rating curve variability *Hydrol. Sci. J.* **45** 221–36

Coss S, Durand M, Yi Y, Jia Y, Guo Q, Tuozzolo S, Shum C K, Allen G H, Calmant S and Pavelsky T 2020 Global river radar altimetry time series (GRRATS): new river elevation earth science data records for the hydrologic community *Earth Syst. Sci. Data* **12** 137–50

Crochemore L, Isberg K, Pimentel R, Pineda L, Hasan A and Arheimer B 2020 Lessons learnt from checking the quality of openly accessible river flow data worldwide *Hydrol. Sci. J.* **65** 699–711

Dawadi S and Ahmad S 2012 Changing climatic conditions in the Colorado River Basin: implications for water resources management *J. Hydrol.* **430–431** 127–41

deFrasson R P M *et al* 2021 Exploring the factors controlling the error characteristics of the surface water and ocean topography mission discharge estimates *Water Resour. Res* **57** e2020WR028519

Dingman S L 2007 Analytical derivation of at-a-station hydraulic–geometry relations *J. Hydrol.* **334** 17–27

Do H X, Gudmundsson L, Leonard M and Westra S 2018 The global streamflow indices and metadata archive (GSIM)—part 1: the production of a daily streamflow archive and metadata *Earth Syst. Sci. Data* **10** 765–85

Drieschova A, Giordano M and Fischhendler I 2008 Governance mechanisms to address flow variability in water treaties *Glob. Environ. Change* **18** 285–95

Durand M *et al* 2016 An intercomparison of remote sensing river discharge estimation algorithms from measurements of river height, width, and slope *Water Resour. Res.* **52** 4527–49

Durand M, Neal J, Rodríguez E, Andreadis K M, Smith L C and Yoon Y 2014 Estimating reach-averaged discharge for the River Severn from measurements of river water surface elevation and slope *J. Hydrol.* **511** 92–104

Elmi O, Tourian M J, Bárdossy A and Sneeuw N 2021 Spaceborne river discharge from a nonparametric stochastic quantile mapping function *Water Resour. Res.* **57** e2021WR030277

ESA 2022 *Copernicus Pod Service File Format Specification* (available at: https://sentinels.copernicus.eu/documents/247904/351187/Copernicus_Sentinels_POD_Service_File_Format_Specification)

Feng D, Gleason C J, Lin P, Yang X, Pan M and Ishitsuka Y 2021 Recent changes to Arctic river discharge *Nat. Commun.* **12** 6917

Feng D, Gleason C J, Yang X and Pavelsky T M 2019 Comparing discharge estimates made via the BAM algorithm in high-order arctic rivers derived solely from optical CubeSat, Landsat, and Sentinel-2 data *Resour. Res.* **55** 7753–71

Findley C V and Rothney J A 2011 *Twentieth-Century World* (Boston, MA: Cengage Learning)

Frasson R P D M, Pavelsky T M, Fonstad M A, Durand M T, Allen G H, Schumann G, Lion C, Beighley R E and Yang X 2019 Global relationships between river width, slope, catchment area, meander wavelength, sinuosity, and discharge *Geophys. Res. Lett.* **46** 3252–62

Gerlak A K, Lautze J and Giordano M 2011 Water resources data and information exchange in transboundary water treaties *Int. Environ. Agreem.: Politics Law Econ.* **11** 179–99

Gerten D, Rost S, von Bloh W and Lucht W 2008 Causes of change in 20th century global river discharge *Geophys. Res. Lett.* **35** L20405

Getirana A C V and Peters-Lidard C 2013 Estimating water discharge from large radar altimetry datasets *Hydrol. Earth Syst. Sci.* **17** 923–33

Gleason C J 2015 Hydraulic geometry of natural rivers: a review and future directions *Prog. Phys. Geogr. Earth Environ.* **39** 337–60

Gleason C J and Durand M 2020 Remote sensing of river discharge: a review and a framing for the discipline *Remote Sens.* **12** 1107

Gorelick N, Hancher M, Dixon M, Ilyushchenko S, Thau D and Moore R 2017 Google earth engine: planetary-scale geospatial analysis for everyone *Remote Sens. Environ.* **202** 18–27

Gourley J J *et al* 2013 A unified flash flood database across the United States *Bull. Am. Meteorol. Soc.* **94** 799–805

Gudmundsson L, Do H X, Leonard M and Westra S 2018 The global streamflow indices and metadata archive (GSIM)—part 2: quality control, time-series indices and homogeneity assessment *Earth Syst. Sci. Data* **10** 787–804

Gupta H V, Kling H, Yilmaz K K and Martinez G F 2009 Decomposition of the mean squared error and NSE performance criteria: implications for improving hydrological modelling *J. Hydrol.* **377** 80–91

Hannah D M, Demuth S, van Lanen H A J, Looser U, Prudhomme C, Rees G, Stahl K and Tallaksen L M 2011 Large-scale river flow archives: importance, current status and future needs *Hydrol. Process.* **25** 1191–200

Harrigan S, Zsoter E, Alfieri L, Prudhomme C, Salamon P, Wetterhall F, Barnard C, Cloke H and Pappenberger F 2020 GloFAS-ERA5 operational global river discharge reanalysis 1979–present *Earth Syst. Sci. Data* **12** 2043–60

Henck A C, Montgomery D R, Huntington K W and Liang C 2010 Monsoon control of effective discharge, Yunnan and Tibet *Geology* **38** 975–8

Hou J, van Dijk A I J M, Renzullo L J and Vertessy R A 2018 Using modelled discharge to develop satellite-based river gauging: a case study for the Amazon Basin *Hydrol. Earth Syst. Sci.* **22** 6435–48

Huang C, Chen Y, Zhang S and Wu J 2018 Detecting, extracting, and monitoring surface water from space using optical sensors: a review *Rev. Geophys.* **56** 333–60

Ignatenko V, Laurila P, Radius A, Lamentowski L, Antropov O and Muff D 2020 ICEYE microsatellite SAR constellation status update: evaluation of first commercial imaging modes *IEEE Int. Symp. on Geoscience and Remote Sensing (IGARSS)* (*2020*) pp 3581–4

India Water Resources Information System 2022 *India Water Resources Information System* (available at: https://indiawris.gov.in/wris/#/)

Ishitsuka Y, Gleason C J, Hagemann M W, Beighley E, Allen G H, Feng D, Lin P, Pan M, Andreadis K and Pavelsky T M 2021 Combining optical remote sensing, McFLI discharge estimation, global hydrologic modelling, and data assimilation to improve daily discharge estimates across an entire large watershed *Water Resour. Res.* **57** e2020WR027794

Japanese Water Information System 2022 *Ministry of Land, Infrastructure, Transport and Tourism* (available at: www.mlit.go.jp/en/)

Ju J and Roy D P 2008 The availability of cloud-free Landsat ETM+ data over the conterminous United States and globally *Remote Sens. Environ.* **112** 1196–211

King M D, Platnick S, Menzel W P, Ackerman S A and Hubanks P A 2013 Spatial and temporal distribution of clouds observed by MODIS onboard the terra and aqua satellites *IEEE Trans. Geosci. Remote Sens.* **51** 3826–52

Knoben W J M, Freer J E and Woods R A 2019 Technical note: inherent benchmark or not? Comparing Nash–Sutcliffe and Kling–Gupta efficiency scores *Hydrol. Earth Syst. Sci.* **23** 4323–31

Kouraev A V, Zakharova E A, Samain O, Mognard N M and Cazenave A 2004 Ob' river discharge from TOPEX/Poseidon satellite altimetry (1992–2002) *Remote Sens. Environ.* **93** 238–45

Krabbenhoft C A *et al* 2022 Assessing placement bias of the global river gauge network *Nat. Sustain.* **5** 1–7

Kulu E 2021 Satellite constellations—2021 industry survey and trends *Small Satellite Conf.* (*Logan, Utah*) (available at: https://digitalcommons.usu.edu/smallsat/2021/all2021/218/)

Kumar M, Kumari A, Kushwaha D P, Kumar P, Malik A, Ali R and Kuriqi A 2020 Estimation of daily stage–discharge relationship by using data-driven techniques of a Perennial River, India *Sustainability* **12** 7877

Larnier K, Monnier J, Garambois P-A and Verley J 2021 River discharge and bathymetry estimation from SWOT altimetry measurements *Inverse Problems Sci. Eng.* **29** 759–89

Leopold L B and Maddock T 1953 *The Hydraulic Geometry of Stream Channels and Some Physiographic Implications* (Washington, DC: U.S. Government Printing Office) (https://doi.org/10.3133/pp252)

Lewis L A 1966 The adjustment of some hydraulic variables at discharges less than one CFS *Prof. Geogr.* **18** 230–4

Lin P *et al* 2019 Global reconstruction of naturalized river flows at 2.94 million reaches *Water Resour. Res.* **55** 6499–516

Linke S *et al* 2019 Global hydro-environmental sub-basin and river reach characteristics at high spatial resolution *Sci. Data* **6** 283

Mersel M K, Smith L C, Andreadis K M and Durand M T 2013 Estimation of river depth from remotely sensed hydraulic relationships *Water Resour. Res.* **49** 3165–79

Milly P C D and Dunne K A 2020 Colorado River flow dwindles as warming-driven loss of reflective snow energizes evaporation *Science* **367** 1252–5

Murphy EC 1904 Accuracy of stream measurements *US Gov. Print. Off* 95 U.S. Geological Survey (https://doi.org/10.3133/wsp95)

Nash J E and Sutcliffe J V 1970 River flow forecasting through conceptual models part I—a discussion of principles *J. Hydrol.* **10** 282–90

National Water Model 2016 *National Water Model* (available at: https://water.noaa.gov/about/nwm)

Neigh C 2021 *Landsat 5* (available at: https://landsat.gsfc.nasa.gov/satellites/landsat-5/) (https://doi.org/10.1038/s41467-021-24253-y)

Nielsen K, Zakharova E, Tarpanelli A, Andersen O B and Benveniste J 2022 River levels from multi mission altimetry, a statistical approach *Remote Sens. Environ.* **270** 112876

Paris A, de Paiva R D, da Silva J S, Moreira D M, Calmant S, Garambois P-A, Collischonn W, Bonnet M-P and Seyler F 2016 Stage-discharge rating curves based on satellite

altimetry and modeled discharge in the Amazon basin *Water Resour. Res.* **52** 3787–814

Pavelsky T M 2014 Using width-based rating curves from spatially discontinuous satellite imagery to monitor river discharge *Hydrol. Process.* **28** 3035–40

Remo J W F, Carlson M and Pinter N 2012 Hydraulic and flood-loss modeling of levee, floodplain, and river management strategies, Middle Mississippi River, USA *Nat. Hazards* **61** 551–75

Riggs R M, Allen G H, David C H, Lin P, Pan M, Yang X and Gleason C 2022 RODEO: an algorithm and Google earth engine application for river discharge retrieval from Landsat *Environ. Model. Softw.* **148** 105254

Rosen P A, Kim Y, Kumar R, Misra T, Bhan R and Sagi V R 2017 Global persistent SAR sampling with the NASA-ISRO SAR (NISAR) mission *IEEE National Conf. on Radar* (*Seattle, Washington*, *2017*) *2017 IEEE Radar Conf. (Radarconf)* pp 0410–4

Schmidt A H, Montgomery D R, Huntington K W and Liang C 2011 The question of communist land degradation: new evidence from local erosion and basin-wide sediment yield in Southwest China and Southeast Tibet *Ann. Assoc. Am. Geogr.* **101** 477–96

Smith L C 1997 Satellite remote sensing of river inundation area, stage, and discharge: a review *Hydrol. Process.* **11** 1427–39

Smith L C and Pavelsky T M 2008 Estimation of river discharge, propagation speed, and hydraulic geometry from space: Lena River, Siberia *Water Resour. Res.* **44** W03427

Spain Anuario de Aforos 2022 *Anuario de Aforos—Anuario de Aforos Digital—datos.gob.es* (available at: http://datos.gob.es/es/catalogo/e00125801-anuario-de-aforos/resource/4836b826-e7fd-4a41-950c-89b4eaea0279)

Stringham C, Farquharson G, Castelletti D, Quist E, Riggi L, Eddy D and Soenen S 2019 The Capella X-band SAR constellation for rapid imaging *2019 IEEE Int. Symp. on Geoscience and Remote Sensing (IGARSS)* (*Yokohama, Japan*) pp 9248–51

Tarpanelli A, Brocca L, Lacava T, Melone F, Moramarco T, Faruolo M, Pergola N and Tramutoli V 2013 Toward the estimation of river discharge variations using MODIS data in ungauged basins *Remote Sens. Environ.* **136** 47–55

Tarpanelli A and Domeneghetti A 2021 Flow duration curves from surface reflectance in the near infrared band *Appl. Sci.* **11** 3458

Thailand Royal Irrigation Department 2022 *RID River Discharge Data* (available at: http://hydro.iis.u-tokyo.ac.jp/GAME-T/GAIN-T/routine/rid-river/disc_d.html)

The Global Runoff Data Centre 2022 The global runoff data centre *GRDC Data Portal* (available at: https://portal.grdc.bafg.de/applications/public.html?publicuser=PublicUser)

Tourian M J, Schwatke C and Sneeuw N 2017 River discharge estimation at daily resolution from satellite altimetry over an entire river basin *J. Hydrol.* **546** 230–47

Tourian M J, Sneeuw N and Bárdossy A 2013 A quantile function approach to discharge estimation from satellite altimetry (ENVISAT) *Water Resour. Res* **49** 4174–86

U.S. Geological Survey 2018 U.S. Geological Survey *Landsat Collections* (https://doi.org/10.3133/fs20183049)

U.S. Geological Survey 2019 *Gages Through the Ages* (available at: https://labs.waterdata.usgs.gov/visualizations/gages-through-the-ages)

U.S. Geological Survey 2022 USGS current water data for the nation *U.S. Geological Survey* (available at: https://waterdata.usgs.gov/nwis/rt)

Wulder M A *et al* 2019 Current status of Landsat program, science, and applications *Remote Sens. Environ.* **225** 127–47

Yang X, Pavelsky T M, Allen G H and Donchyts G 2020 RivWidthCloud: an automated Google earth engine algorithm for river width extraction from remotely sensed imagery *IEEE Geosci. Remote Sens. Lett.* **17** 217–21

Yang Y *et al* 2021 Global reach-level 3-hourly river flood reanalysis (1980–2019) *Bull. Am. Meteorol. Soc.* **102** E2086–105

Zhao F *et al* 2017 The critical role of the routing scheme in simulating peak river discharge in global hydrological models *Environ. Res. Lett.* **12** 075003